# GEOMETRICALLY NON-LINEAR ANALYSIS OF SHELLS

## ANDRZEJ AMBROZIAK

*Department of Structural Mechanics and Bridges Structures,*
*Faculty of Civil and Environmental Engineering,*
*Gdansk University of Technology,*
*Narutowicza 11/12, 80-952 Gdansk, Poland*
*ambrozan@pg.gda.pl*

**Abstract:** The work's aim has been to verify the suitability of commercial engineering software for geometrically non-linear analysis of shell structures. The paper deals with static, geometrically non-linear analysis of shells made of isotropic materials. The Finite Element Method (FEM) has been chosen to solve the problem. The results of the ROBOBAT Robot Millennium v. 19.0 and MSC.Marc v. 2005r2 commercial software are compared with the literature results.

**Keywords:** FEM, locking, shell, geometric non-linear

## 1. Introduction

The Finite Element Method (FEM) is an approximate method. Before detailed numerical calculations of the structure are performed, it is necessary to assume a proper division of construction of finite elements. Additionally, we have to be sure that the applied type of finite element is error-free. One of the most common problems in the description of finite elements is locking. A number of concepts have been developed to define and explain this effect. The term reflects a graphical perception that the structure locks itself against deformations. Thus, locking means the effect of a reduced rate of convergence with reference to the critical parameter. Infinite growth of the parameter may even make its convergence tend to zero.

## 2. Locking effects

It is possible to specify three types of locking: membrane, shear and volumetric locking. It is worth pointing out that locking effects are of numerical background; they are usually connected with a low interpolation rule of the Lagrange type (see *e.g.* Chróścielewski *et al.* [1]). Volumetric locking is related to Poisson's ratio, $\nu$, and so sometimes referred to as Poisson locking. The nature of the volumetric locking is simple to explain if the bulk modulus is taken as the critical parameter:

$$\kappa = \frac{E}{3 - 6 \cdot \nu}.$$

(1)

We can see that this effect occurs only in the incompressible case, for $\nu = 0.5$, because

$$\lim_{\nu \to 0.5} \kappa = \infty. \tag{2}$$

Thus the Poisson ratio of $\nu = 0$ gives no volumetric locking. The effect becomes more pronounced when $\nu = 0.5$.

Various approaches have been developed to avoid volumetric locking. Nagtegaal *et al.* [2] used special crossed patch arrangements of linear triangular elements. Hughes [3] proposed applying the B-bar approach to linear quadrilateral elements. Simo and Rifai [4] applied the enhanced assumed strain approach. Rong and Lu [5] described generalized mixed variation principles to solve ill-conditioned problems in computational mechanics. Wells *et al.* [6] proposed a *p*-adaptive scheme to prevent volumetric locking in low-order elements. Additionally, the selective reduced integration method (see *e.g.* Naylor [7], Malkus and Hughes [8]), the penalty method (see *e.g.* Jankovich *et al.* [9], Oden and Kikuchi [10]) and mixed formulation methods (see *e.g.* Taylor *et al.* [11], Argyris *et al.* [12], Simo *et al.* [13], Canga and Becker [14]) have been used to counteract volumetric locking.

Plate and shell elements of shear-deformable beams are subjected to transverse shear locking. This kind of locking occurs in three-dimensional solid elements and can be observed in modelling of thin-walled structures. Transverse shear locking is one of the most important locking effects (see *e.g.* Belytschko and Bachrach [15], Koh and Kikuchi [16]), it slows down the rate of convergence and essentially precludes analysis in practical applications with a reasonable amount of numerical effort. As the error oscillates within an element, simple smoothing often helps to significantly improve the stresses.

In the early 1970's, reduced and selective reduced integration techniques were proposed and investigated in order to prevent the shear locking problem (see *e.g.* Zienkiewicz *et al.* [17], Pawsey and Clough [18] and Hughes *et al.* [19]). Alternative techniques followed: Stolarski and Chiang [20] and Simo and Rifai [4] applied enhanced assumed strain methods, Pinsky and Jasti [21] and Franca and Farhat [22] used bubble function methods, while Bathe and Dvorkin [23] and Belytschko *et al.* [24] applied hybrid-mixed methods.

A quadrature rule for an eight-node solid finite element was presented by Olovsson *et al.* [25]. The proposed method of averaging shear strains resulted in a reduction of locking effects eliminating them completely in the analysis of rectangular elements. It is worth pointing out that no zero-energy modes occurred in the proposed formulation. Ozkul and Ture [26] presented two simple plate-bending elements based on the Mindlin theory to analyse both moderately thick and thin plates. In order to test shear locking, the results obtained from the Mindlin plate analysis using four- or eight-node elements with full, reduced and selectively reduced integration were compared with the exact classical thin plate solution. Vermeulen and Heppler [27] explained the notion of shear locking in general terms, applying the B-spline field approximation method to two forms of the Timoshenko beam model. Rong and Lu [28] applied the generalized mixed variation principles to shear locking of the Reissner plate theory and the Timoshenko beam theory. Laulusa and Reddy [29] developed a displacement beam finite element model based on non-linear kinematics of a pre-twisted composite

beam. The author used a reduced and selective integration technique to prevent the shear and extensional locking. Chróścielewski *et al.* [30] proposed a 4-node C$^0$ shell element with the drilling degree of freedom. In order to avoid the locking phenomena, the assumed natural strain technique and the enhanced assumed strain technique were proposed for shear locking and membrane locking, respectively.

Membrane locking occurs in curved beam and shell elements. The term „membrane locking" denotes a stiffening effect that occurs when pure bending deformations (the so-called inextensional bending) are accompanied by parasitic membrane stresses. It is sometimes misused with reference to shear locking and volumetric locking as these affect the membrane part of shell elements.

Shell elements, especially considering nine-node quadrilaterals, which are free from membrane locking, have been developed successfully on the basis of the assumed natural strain method (see *e.g.* MacNeal [31], Park and Stanley [32]). The enhanced assumed strain method is often used in the case of bilinear elements to improve the membrane part of shell elements (see *e.g.* Simo and Rifai [4], Braess [33] and Witkowski [34]). Koschnick *et al.* [35] focused on the application of the discrete strain gap method to the problem of membrane locking in finite beam and shell elements. Choi *et al.* [36] investigated the membrane locking problem in finite element computations of thin shells. A refined triangular plate element non-linear was developed for geometric non-linear analysis by Jufen and Wanji [37]. The membrane locking phenomena were considered in their paper by introducing a special element displacement function into the geometric stiffness matrix. In the context of beam elements, shear locking and membrane locking were explained by Yunhua [38] in the framework of the field consistence approach. Hakula *et al.* [39] demonstrated some typical characteristics of linear shell problems (scale resolution and locking) and presented, both theoretically and experimentally, the benefits of higher-order finite elements in shell problems. Choi and Lee [40] presented an efficient scheme to remove membrane locking of 4-node quadrilateral flat shell elements using various non-conforming modes. Witkowski [34] developed a family of finite elements within the framework of a non-linear 6-parameter shell theory, studied in the context of locking phenomena.

## 3. The programs

A geometrically non-linear finite element analysis has been performed. The MSC.Marc system and the Robot Millennium program were applied in the numerical calculations.

The MSC.Marc is a non-linear finite element program. The system's great advantage is the possibility of introducing a large number of open, user-modifiable subroutines. [41], [42] and [43] are examples of the use of UVSCPL subroutines to implement the elasto-viscoplastic Chaboche and Bodner-Partom models into the MSC.Marc system. At the present stage of research only standard procedures were used.

The ROBOBAT Robot Millennium system (RM) is a computer program integrated with the graphical environment designed for modelling, analysis and dimen-
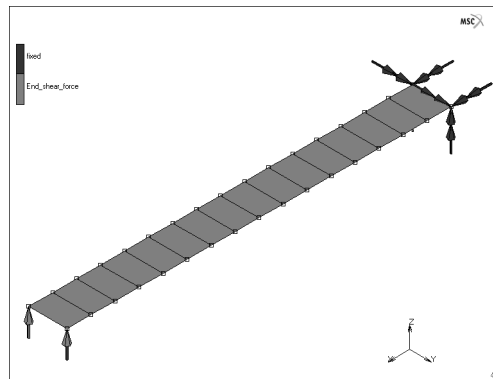
**Figure 1.** Initial geometry and boundary conditions for cantilever subjected to end shear force
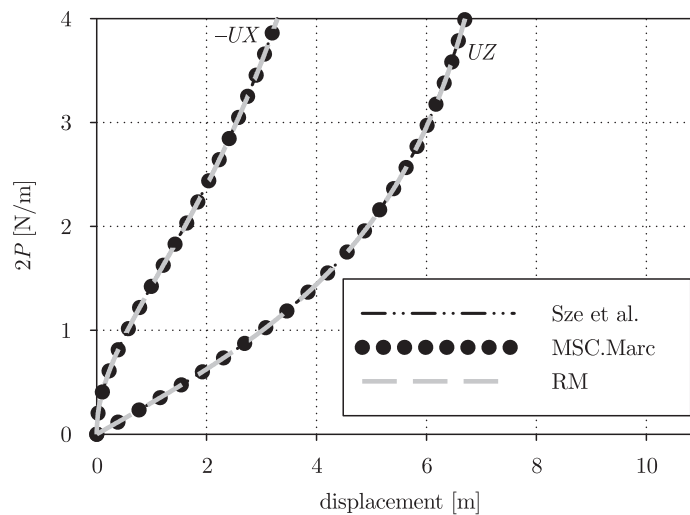


**Figure 2.** Load-displacement curves for the cantilever subjected to end shear force

sioning of various structures. National versions of this software are elaborated in several countries including national standards.

Geometrically non-linear analysis with the options of small strains and linear isotropic elastic model has been selected in both of these commercial programs. A group of reference results were taken from Sze *et al.* [44] (Test 1, Test 2 and Test 3) and Chróścielewski [45] (Test 3). It should be noted that Sze *et al.* [44] worked in the ABAQUS system with S4R reduced-integrated curved shell elements. The present author used a bilinear thin-shell element (Element 139, see [46]) in the MSC.Marc analysis and 4-node shell elements in the ROBOBAT Robot Millennium calculations.

## 4. Benchmark tests

### 4.1. Test 1 – A cantilever subjected to the end shear force

The first benchmark test was performed for a cantilever subjected to the end shear force (see Figure 1). $E = 1.2\,\mathrm{MPa}$ and $\nu = 0.0$ were as assumed parameters for the

**Table 1.** Displacement of cantilever subjected to end shear force

| $2P$ | MSC.Marc | | Robot Millennium | | Sze *et al.* [44] | |
|---|---|---|---|---|---|---|
| [N/m] | $-UX_{\text{tip}}$ [m] | $UZ_{\text{tip}}$ [m] | $-UX_{\text{tip}}$ [m] | $UZ_{\text{tip}}$ [m] | $-UX_{\text{tip}}$ [m] | $UZ_{\text{tip}}$ [m] |
| 0.0 | 0.000 | 0.000 | 0.000 | 0.000 | 0.000 | 0.000 |
| 0.2 | 0.026 | 0.663 | 0.026 | 0.663 | 0.026 | 0.663 |
| 0.4 | 0.103 | 1.309 | 0.103 | 1.310 | 0.103 | 1.309 |
| 0.6 | 0.225 | 1.923 | 0.225 | 1.924 | 0.224 | 1.922 |
| 0.8 | 0.381 | 2.494 | 0.381 | 2.495 | 0.381 | 2.493 |
| 1.0 | 0.564 | 3.017 | 0.564 | 3.018 | 0.563 | 3.015 |
| 1.2 | 0.763 | 3.490 | 0.764 | 3.492 | 0.763 | 3.488 |
| 1.4 | 0.972 | 3.915 | 0.973 | 3.917 | 0.971 | 3.912 |
| 1.6 | 1.185 | 4.295 | 1.186 | 4.297 | 1.184 | 4.292 |
| 1.8 | 1.397 | 4.633 | 1.399 | 4.636 | 1.396 | 4.631 |
| 2.0 | 1.605 | 4.935 | 1.607 | 4.938 | 1.604 | 4.933 |
| 2.2 | 1.808 | 5.205 | 1.810 | 5.208 | 1.807 | 5.202 |
| 2.4 | 2.004 | 5.447 | 2.006 | 5.449 | 2.002 | 5.444 |
| 2.6 | 2.191 | 5.663 | 2.194 | 5.666 | 2.190 | 5.660 |
| 2.8 | 2.371 | 5.858 | 2.374 | 5.861 | 2.370 | 5.855 |
| 3.0 | 2.543 | 6.034 | 2.545 | 6.037 | 2.541 | 6.031 |
| 3.2 | 2.707 | 6.194 | 2.709 | 6.196 | 2.705 | 6.190 |
| 3.4 | 2.863 | 6.339 | 2.865 | 6.341 | 2.861 | 6.335 |
| 3.6 | 3.012 | 6.471 | 3.014 | 6.473 | 3.010 | 6.467 |
| 3.8 | 3.154 | 6.592 | 3.156 | 6.593 | 3.151 | 6.588 |
| 4.0 | 3.288 | 6.702 | 3.290 | 6.704 | 3.286 | 6.698 |
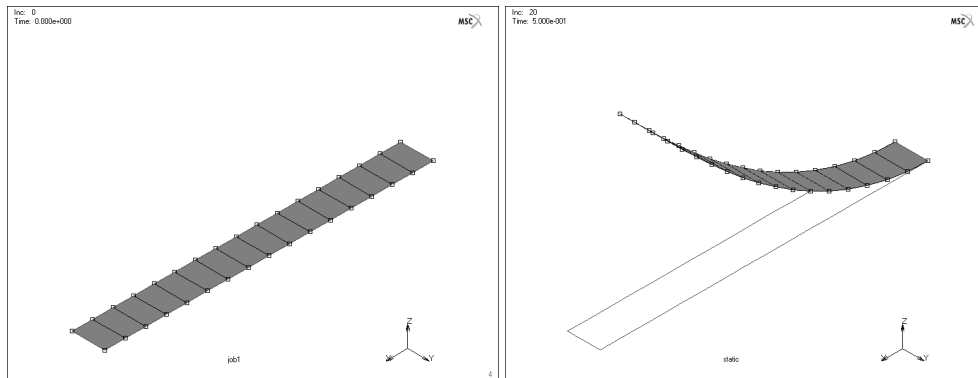


**Figure 3.** Undeformed ($P = 0$, left) and deformed ($P = 0.5P_{\text{max}}$, right) configurations of the cantilever subjected to end shear force – MSC.Marc results

isotropic elastic model: and the following dimensions: width $b = 1$ m, length $l = 10$ m and thickness $t = 0.1$ m.

The curves of vertical and horizontal tip displacement versus end shear forces are presented in Figure 2. The deformation process of a cantilever subjected to the end shear force is shown in Figures 3 and 4. Good agreement of displacement versus end shear force has been obtained from numerical and reference calculations (see Table 1).

### 4.2. Test 2 – A cantilever subjected to the end moment

In this example a cantilever has been subjected to the free end moment (see Figure 5). The following parameters were assumed: $E = 1.2$ MPa, $\nu = 0.0$, $b = 1$ m, $t = 0.1$ m. The cantilever length was $l = 12.0$ m. The load-end moment diagram is shown in Figure 6, while the deformation process is presented Figures 7–9. The numerical results of tip displacements are listed in Table 2. The load-displacement functions
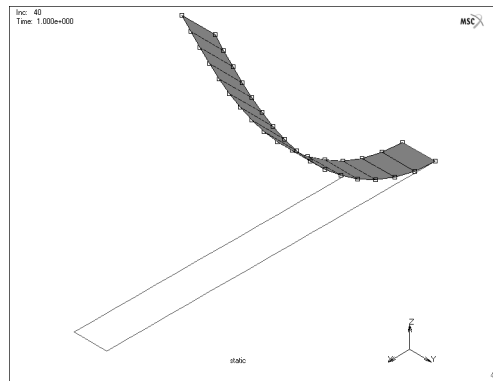
**Figure 4.** Deformed configurations ($P = P_{\max}$) of the cantilever subjected to end shear force – MSC.Marc results
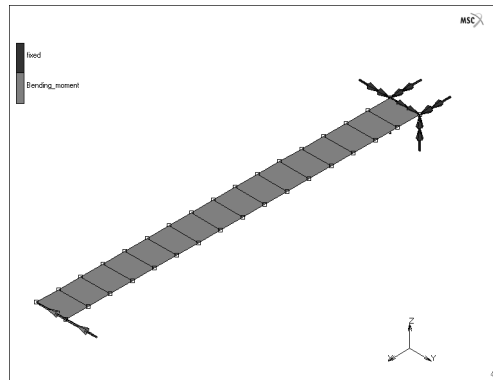


**Figure 5.** Initial geometry and boundary for cantilever subjected to end bending moment

obtained from the two investigated computer programs have yielded similar results in the considered range of loading.

In this example it is possible to calculate the exact solution (see Table 2) based on the beam theory, assuming pure bending in the $X$–$Z$ plane, constant stiffness $EJ^Y$ and the initial configuration analysis of $s = X$. Thus, according to [45]:

$$
\left.\begin{array}{l}
\dfrac{1}{\rho^X(s)} = \dfrac{d\varphi}{ds} = \dfrac{M^Y(s)}{E I^Y(s)} = \text{const} \\[2mm]
\dfrac{dZ}{ds} = \dfrac{1}{\rho^X}\dfrac{dZ}{d\varphi} = \sin\varphi \\[2mm]
\dfrac{dX}{ds} = \dfrac{1}{\rho^X}\dfrac{dX}{d\varphi} = \cos\varphi
\end{array}\right\}
\Rightarrow
\begin{cases}
Z(s) = \rho^X(1 - \cos\varphi(s)) \\[2mm]
X(s) = \rho^X \sin\varphi(s)
\end{cases}
\tag{3}
$$

### 4.3. Test 3 – A hemispherical shell subjected to alternating radial forces

A hemispherical shell with an $18°$ circular cut-out at the pole has been investigated (see Figure 10). The shell was loaded by four alternating radial point forces. The shell parameters were as follows: the elastic modulus of $E = 68.25\,\text{MPa}$, Poisson's ratio of $\nu = 0.3$, a mean radius of $R = 10\,\text{m}$ and the thickness of $t = 0.04\,\text{m}$.
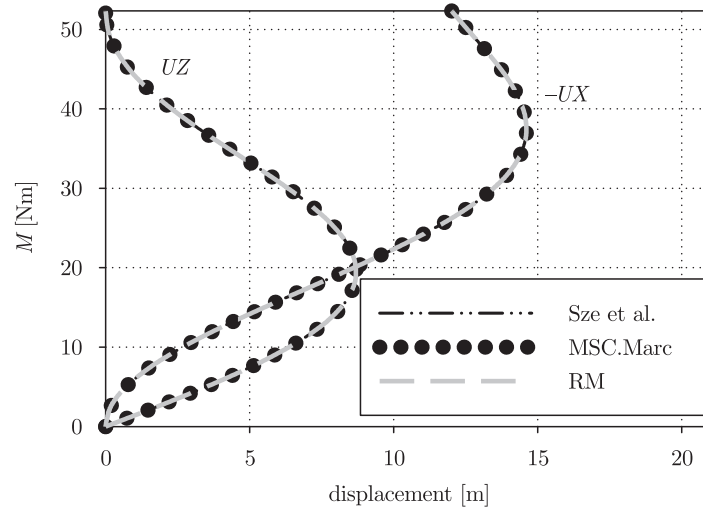
**Figure 6.** Load-displecement curves for the cantilever subjected to end bending moment

**Table 2.** Displacement of cantilever subjected to end bending moment

| $M$ [Nm] | MSC.Marc $16 \times 1$ | | Robot Millennium $16 \times 1$ | | Sze *et al.* [44] $16 \times 1$ | | Exact solution | |
|---|---|---|---|---|---|---|---|---|
| | $-UX_{\text{tip}}$ [m] | $UZ_{\text{tip}}$ [m] | $-UX_{\text{tip}}$ [m] | $UZ_{\text{tip}}$ [m] | $-UX_{\text{tip}}$ [m] | $UZ_{\text{tip}}$ [m] | $-UX_{\text{tip}}$ [m] | $UZ_{\text{tip}}$ [m] |
| 0.000 | 0.000 | 0.000 | 0.000 | 0.000 | 0.000 | 0.000 | 0.000 | 0.000 |
| 2.618 | 0.196 | 1.869 | 0.196 | 1.870 | 0.196 | 1.870 | 0.196 | 1.870 |
| 5.236 | 0.773 | 3.646 | 0.773 | 3.648 | 0.773 | 3.648 | 0.774 | 3.648 |
| 7.854 | 1.696 | 5.248 | 1.698 | 5.249 | 1.698 | 5.249 | 1.699 | 5.248 |
| 10.472 | 2.913 | 6.599 | 2.916 | 6.600 | 2.916 | 6.600 | 2.918 | 6.598 |
| 13.090 | 4.354 | 7.641 | 4.357 | 7.642 | 4.357 | 7.643 | 4.361 | 7.639 |
| 15.708 | 5.938 | 8.338 | 5.942 | 8.338 | 5.942 | 8.338 | 5.945 | 8.333 |
| 18.326 | 7.577 | 8.672 | 7.582 | 8.671 | 7.582 | 8.671 | 7.585 | 8.664 |
| 20.944 | 9.186 | 8.649 | 9.190 | 8.646 | 9.191 | 8.646 | 9.194 | 8.637 |
| 23.562 | 10.682 | 8.295 | 10.686 | 8.292 | 10.687 | 8.291 | 10.688 | 8.281 |
| 26.180 | 11.996 | 7.657 | 11.998 | 7.653 | 12.000 | 7.652 | 12.000 | 7.639 |
| 28.798 | 13.073 | 6.795 | 13.074 | 6.790 | 13.075 | 6.788 | 13.073 | 6.775 |
| 31.416 | 13.875 | 5.779 | 13.875 | 5.772 | 13.875 | 5.772 | 13.871 | 5.758 |
| 34.034 | 14.385 | 4.685 | 14.383 | 4.678 | 14.384 | 4.678 | 14.377 | 4.665 |
| 36.652 | 14.606 | 3.590 | 14.603 | 3.582 | 14.603 | 3.583 | 14.595 | 3.571 |
| 39.270 | 14.561 | 2.562 | 14.556 | 2.557 | 14.556 | 2.556 | 14.546 | 2.546 |
| 41.888 | 14.287 | 1.661 | 14.281 | 1.657 | 14.280 | 1.656 | 14.270 | 1.650 |
| 44.506 | 13.834 | 0.933 | 13.828 | 0.932 | 13.826 | 0.931 | 13.818 | 0.926 |
| 47.124 | 13.263 | 0.408 | 13.256 | 0.408 | 13.254 | 0.407 | 13.247 | 0.405 |
| 49.742 | 12.634 | 0.097 | 12.629 | 0.100 | 12.625 | 0.099 | 12.621 | 0.098 |
| 52.360 | 12.008 | $-0.004$ | 12.005 | 0.001 | 12.000 | 0.000 | 12.000 | 0.000 |

The MSC.Marc and RM results are convergent and comparable with the results obtained by Sze *et al.* [44] (*cf.* Figure 11 and Table 3). The shell deformation process under radial point forces is shown in Figures 12–14.

## 5. Conclusions and final remarks

Common benchmark problems of geometric non-linear analysis of shells have been presented in this study. Membrane, shear and volumetric locking phenomena
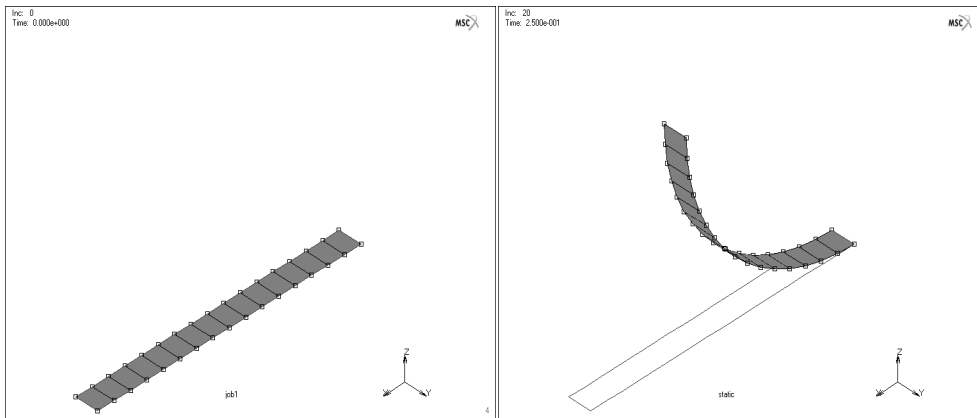
**Figure 7.** Deformation process of the cantilever subjected to end bending moment
for $M = 0$ (left) and $M = 0.25M_{\max}$ (right) – MSC.Marc results
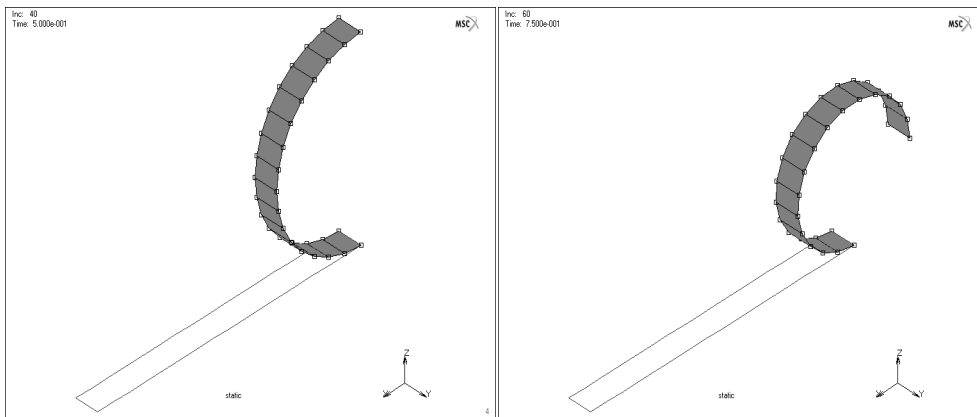


**Figure 8.** Deformation process of the cantilever subjected to end bending moment
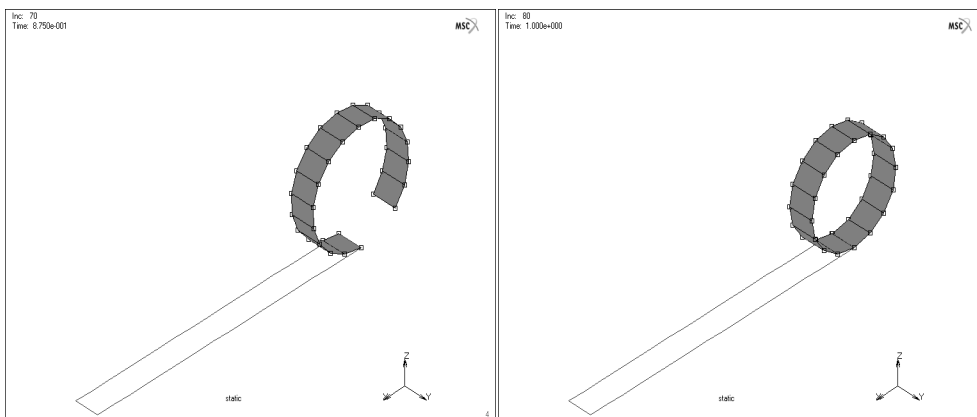for $M = 0.5M_{\max}$ (left) and $M = 0.75M_{\max}$ (right) – MSC.Marc results



**Figure 9.** Deformation process of the cantilever subjected to end bending moment
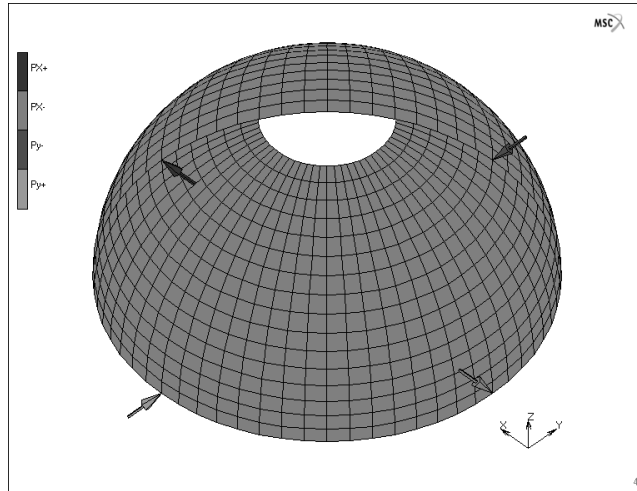for $M = 0.875M_{\max}$ (left) and $M = M_{\max}$ (right) – MSC.Marc results

**Figure 10.** Initial geometry and boundary conditions for the hemispherical shell
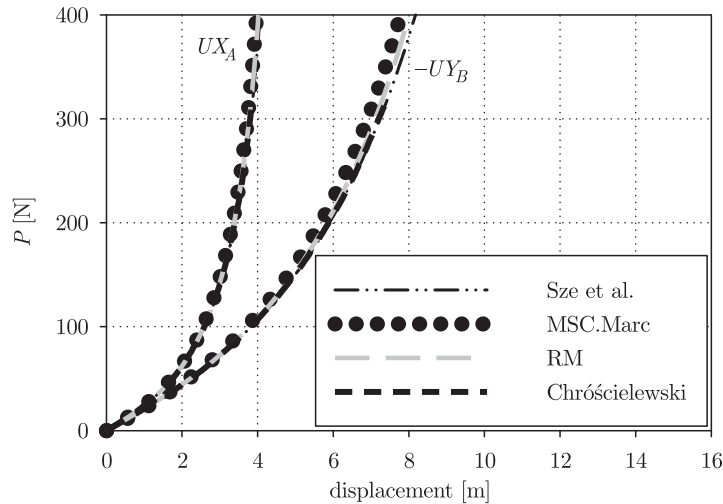


**Figure 11.** Load-deflection curves for the hemispherical shell subjected to radial forces

have been described and investigated. A geometrically non-linear analysis of shell structures has been carried out, using two commercial software systems, the MSC.Marc program and Robot Millennium.

This paper is an introduction to comprehensive investigation of geometrically non-linear analysis of shells. For detailed studies of geometrically non-linear analysis of shells the reader is referred to Chróścielewski *et al.* [1] and [47], Lubowiecka [48], Lubowiecka and Chróścielewski [49], Chróścielewski and Witkowski [34], where a family of finite elements is developed for static and dynamic problems, in the framework of the non-linear 6-parameter shell theory.

### Acknowledgements

**Table 3.** Displacement of the hemispherical shell subjected to radial forces

| $P$ [N] | MSC.Marc $16 \times 16$ | | Robot Millennium $16 \times 16$ | | Sze *et al.* [44] $16 \times 16$ | | Chróścielewski [45] CAM $18 \times 18$ | |
|---|---|---|---|---|---|---|---|---|
| | $UX_A$ [m] | $-UY_B$ [m] | $UX_A$ [m] | $-UY_B$ [m] | $UX_A$ [m] | $-UY_B$ [m] | $UX_A$ [m] | $-UY_B$ [m] |
| 0 | 0.0000 | 0.0000 | 0.0000 | 0.0000 | 0.000 | 0.000 | 0.0000 | 0.0000 |
| 20 | 0.8489 | 0.9423 | 0.8530 | 0.9500 | 0.855 | 0.955 | 0.8550 | 0.9545 |
| 40 | 1.4845 | 1.8013 | 1.4950 | 1.8270 | 1.499 | 1.840 | 1.499 | 1.838 |
| 60 | 1.9443 | 2.5368 | 1.9620 | 2.5830 | 1.969 | 2.604 | 1.969 | 2.600 |
| 80 | 2.2883 | 3.1665 | 2.3120 | 3.2330 | 2.321 | 3.261 | — | — |
| 100 | 2.5562 | 3.7133 | 2.5850 | 3.7990 | 2.596 | 3.833 | 2.596 | 3.827 |
| 120 | 2.7719 | 4.1946 | 2.8040 | 4.2970 | 2.819 | 4.339 | — | — |
| 140 | 2.9500 | 4.6231 | 2.9850 | 4.7410 | 3.002 | 4.790 | — | — |
| 160 | 3.1001 | 5.0080 | 3.1380 | 5.1390 | 3.158 | 5.196 | 3.157 | 5.188 |
| 180 | 3.2285 | 5.3563 | 3.2680 | 5.5000 | 3.291 | 5.565 | — | — |
| 200 | 3.3398 | 5.6734 | 3.3810 | 5.8280 | 3.406 | 5.902 | — | — |
| 220 | 3.4374 | 5.9635 | 3.4800 | 6.1280 | 3.508 | 6.212 | — | — |
| 240 | 3.5237 | 6.2301 | 3.5680 | 6.4040 | 3.598 | 6.497 | 3.597 | 6.488 |
| 260 | 3.6007 | 6.4760 | 3.6460 | 6.6590 | 3.678 | 6.761 | — | — |
| 280 | 3.6699 | 6.7038 | 3.7160 | 6.8940 | 3.750 | 7.006 | — | — |
| 300 | 3.7324 | 6.9153 | 3.7800 | 7.1130 | 3.816 | 7.234 | — | — |
| 320 | 3.7892 | 7.1124 | 3.8370 | 7.3170 | 3.875 | 7.448 | 3.874 | 7.439 |
| 340 | 3.8411 | 7.2966 | 3.8900 | 7.5070 | 3.929 | 7.647 | — | — |
| 360 | 3.8888 | 7.4691 | 3.9380 | 7.6850 | 3.979 | 7.835 | — | — |
| 380 | 3.9328 | 7.6312 | 3.9830 | 7.8520 | 4.0250 | 8.011 | — | — |
| 400 | 3.9735 | 7.7838 | 4.0240 | 8.0100 | 4.067 | 8.178 | — | — |
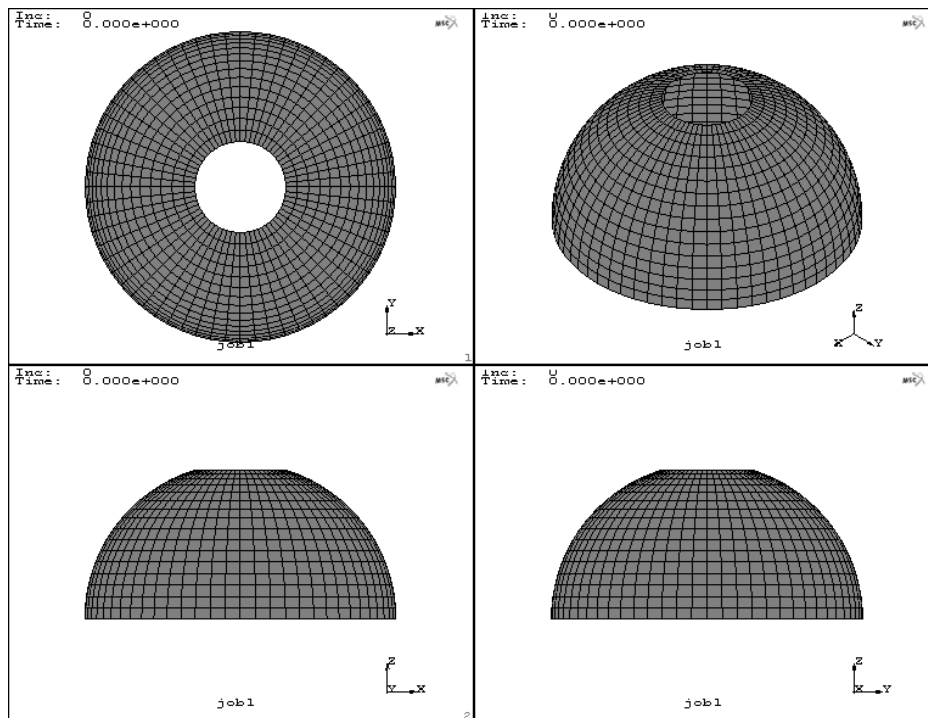


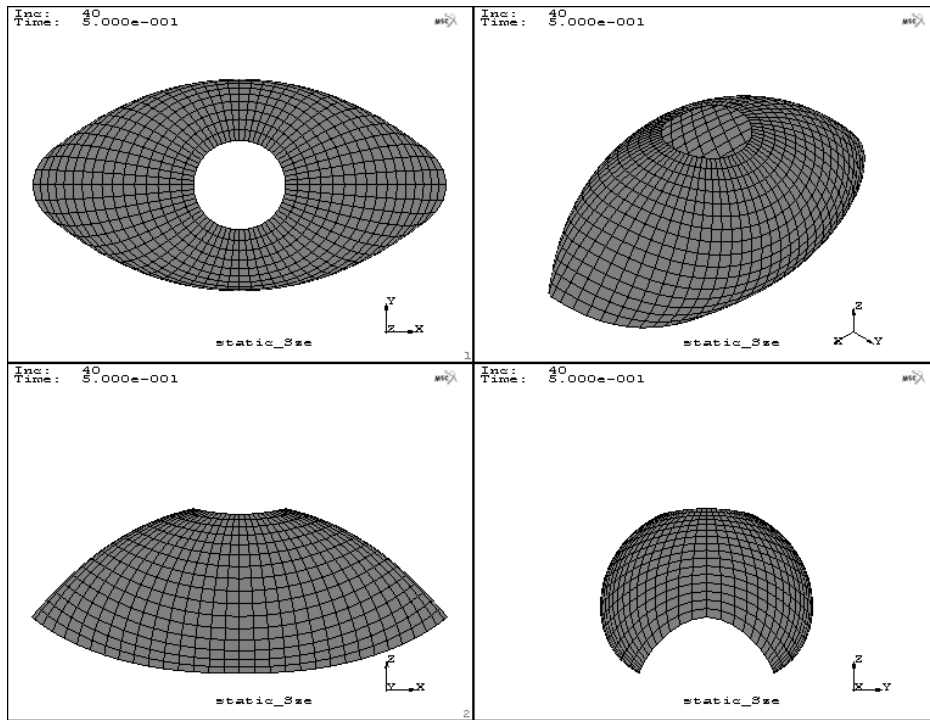**Figure 12.** Deformation of the hemispherical shell – MSC.Marc results, $P = 0$

**Figure 13.** Deformation of the hemispherical shell – MSC.Marc results, $P = 0.5P_{\max}$
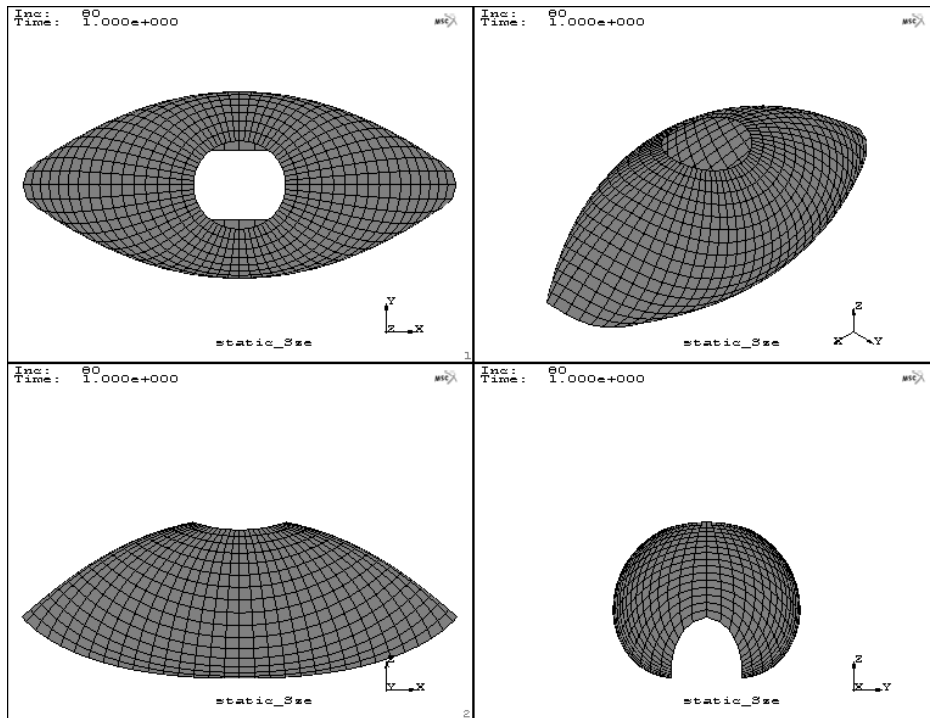


**Figure 14.** Deformation of the hemispherical shell – MSC.Marc results, $P = P_{\max}$

## *References*

[1] Chróścielewski J, Makowski J and Pietraszkiewicz W 2004 *Static and Dynamic of Branched Shells. Nonlinear Theory and Finite Element Methods*, Institute of Fundamental Technological Research, Polish Academy of Science, Warsaw (in Polish)

[2] Nagtegaal J C, Parks D M and Rice J R 1974 *Comp. Methods in Appl. Mech. and Eng.* **4** 153

[3] Hughes T J R 1980 *Int. J. for Num. Methods in Eng.* **15** 1413

[4] Simo J C and Rifai M S 1990 *Int. J. for Num. Methods in Eng.* **29** 1595

[5] Rong T-Y and Lu A-Q 2001 *Comp. Methods in Appl. Mech. and Eng.* **191** 407

[6] Wells G N, Sluys L J and de Borst R 2002 *Comp. Methods in Appl. Mech. and Eng.* **191** 3153

[7] Naylor J 1974 *Int. J. for Num. Methods in Eng.* **8** 443

[8] Malkus D S and Hughes T J R 1978 *Comp. Methods in Appl. Mech. and Eng.* **15** 63

[9] Jankovich E, Leblec F, Durand M and Bercovier M 1981 *Computer & Structures* **14** 385

[10] Oden J T and Kikuchi N 1982 *Int. J. for Num. Methods in Eng.* **18** 701

[11] Taylor R L, Pister K S and Herrmann L R 1968 *Int. J. of Solids and Struct.* **4** 875

[12] Argyris J H, Dunne P C, Angelopoulus T and Bichat B 1974 *Comp. Methods in Appl. Mech. and Eng.* **4** 219

[13] Simo J C, Taylor R L and Pister K S 1985 *Comp. Methods in Appl. Mech. and Eng.* **51** 177

[14] Canga M E and Becker E B 1999 *Comp. Methods in Appl. Mech. and Eng.* **170** 79

[15] Belytschko T and Bachrach W E 1986 *Computer Methods in Appl. Mech. and Eng.* **54** 279

[16] Koh B C and Kikuchi N 1987 *Comp. Methods in Appl. Mech. and Eng.* **65** 1

[17] Zienkiewicz O C, Taylor R L and Too J M 1971 *Int. J. for Num. Methods in Eng.* **3** 275

[18] Pawsey S F and Clough R W 1971 *Int. J. for Num. Methods in Eng.* **3** 575

[19] Hughes T J R, Taylor R L and Kanoknukulchai W 1977 *Int. J. for Num. Methods in Eng.* **11** 1529

[20] Stolarski H K and Chiang M Y M 1989 *Int. J. for Num. Methods in Eng.* **28** 2323

[21] Pinsky P M and Jasti R V 1989 *Int. J. for Num. Methods in Eng.* **28** 1677

[22] Franca L P and Farhat C 1995 *Com. Methods in Appl. Mech. and Eng.* **123** 299

[23] Bathe K-J and Dvorkin E N 1985 *Int. J. for Num. Methods in Eng.* **21** 367

[24] Belytschko T, Liu W K and Ong J S 1987 *Comp. Methods in Appl. Mech. and Eng.* **62** 275

[25] Olovsson L, Simonsson K and Unosson M 2006 *Computer & Structures* **84** 476

[26] Ozkul T A and Ture U 2004 *Thin-Wallded Struct.* **42** 1405

[27] Vermeulen A H and Heppler G R 1998 *Com. Methods in Appl. Mech. and Eng.* **158** 311

[28] Rong T-Y and Lu A-Q 2003 *Comp. Methods in Appl. Mech. and Eng.* **192** 4981

[29] Laulusa A and Reddy J N 2004 *Eng. Struct.* **26** 151

[30] Chróścielewski J, Lubowiecka I and Witkowski W 2005 *Shell Structures: Theory and Applications* (Piertaszkiewicz W and Szymczak C, Eds), Taylor & Francis Group, London, pp. 451–455

[31] Mac Neal R H 1982 *Nuclear Eng. Design* **70** 3

[32] Park K C and Stanley G M 1986 *J. of Appl. Mech.* **53** 278

[33] Braess D 1998 *Comp. Methods in Appl. Mech. and Eng.* **165** 155

[34] Chróścielewski J and Witkowski W 2006 *Int. J. for Num. Methods in Eng.* (in press)

[35] Koschnick F, Bischoff M, Camprubí N and Bletzinger K-U 2005 *Comp. Methods in Appl. Mech. and Eng.* **194** 2444

[36] Choi D, Palma F J, Sanchez-Palenicia E and Vilariño M A 1998 *Math. Modelling and Num. Anal.* **32** 131

[37] Jufen Z and Wanji C 1997 *Computer & Structures* **63** 999

[38] Yunhua L 1998 *Comp. Methods in Appl. Mech. and Eng.* **162** 249

[39] Hakula H, Leino Y and Pitkäranta J 1996 *Comp. Methods in Appl. Mech. and Eng.* **133** 157

[40] Choi C-K and Lee T-Y 2003 *Comp. Method in Appl. Mech. and Eng.* **192** 1961

[41] Ambroziak A 2005 *TASK Quart.* **9** 157

[42] Ambroziak A 2005 *Shell Structures: Theory and Applications* (Pietraszkiewicz W and Szymczak C, Eds), Balkema Proc. and Monographs in Eng., Water and Earth Scs, Taylor & Francis Group, pp. 445–449

[43] Ambroziak A 2005 *TASK Quart.* **4** 167

[44] Sze K Y, Liu X H and Lo S H 2004 *Finite Element in Analysis and Design* **40** 1551

[45] Chróścielewski J 1996 *The Family of $C^0$ Finite Elements in the Nonlinear Six-parameter Shell Theory*, Zeszyty Naukowe Politechniki Gdańskiej, Budownictwo Lądowe **53**, Gdansk (in Polish)

[46] *Users handbook MSC.MARC: Volume B: Element library; Volume D: User subroutines and special routines*, Version 2003, MSC.Software Corporation 2003

[47] Chróścielewski J, Makowski J and Pieraszkiewicz W 2002 *Comp. Assisted Mech. and Eng. Scs* **19** 341

[48] Lubowiecka I 2004 *Integration of Nonlinear Dynamic Equations of Rigid Body and Elastic Shells*, Gdansk University of Technology Press, Gdansk (in Polish)

[49] Lubowiecka I and Chróścielewski J 2002 *Computer & Structures* **80** 891